Irrational exuberance and neural crash warning signals during endogenous experimental market bubbles

Alec Smith[a,1], Terry Lohrenz[b], Justin King[b], P. Read Montague[b,c,1], and Colin F. Camerer[a,1]

[a]Humanities and Social Sciences and Computational and Neural Systems, California Institute of Technology, Pasadena, CA 91125; [b]Virginia Tech Carilion Research Institute, Virginia Tech, Roanoke, VA 24016; and [c]The Wellcome Trust Centre for Neuroimaging, University College London, London WC1N 3BG, United Kingdom

Edited by Jose A. Scheinkman, Columbia University, New York, NY, and approved June 2, 2014 (received for review October 8, 2013)

Groups of humans routinely misassign value to complex future events, especially in settings involving the exchange of resources. If properly structured, experimental markets can act as excellent probes of human group-level valuation mechanisms during pathological overvaluations—price bubbles. The connection between the behavioral and neural underpinnings of such phenomena has been absent, in part due to a lack of enabling technology. We used a multisubject functional MRI paradigm to measure neural activity in human subjects participating in experimental asset markets in which endogenous price bubbles formed and crashed. Although many ideas exist about how and why such bubbles may form and how to identify them, our experiment provided a window on the connection between neural responses and behavioral acts (buying and selling) that created the bubbles. We show that aggregate neural activity in the nucleus accumbens (NAcc) tracks the price bubble and that NAcc activity aggregated within a market predicts future price changes and crashes. Furthermore, the lowest-earning subjects express a stronger tendency to buy as a function of measured NAcc activity. Conversely, we report a signal in the anterior insular cortex in the highest earners that precedes the impending price peak, is associated with a higher propensity to sell in high earners, and that may represent a neural early warning signal in these subjects. Such markets could be a model system to understand neural and behavior mechanisms in other settings where emergent group-level activity exhibits mistaken belief or valuation.

neuroeconomics | asset bubbles | hyperscanning

Asset price bubbles are extended periods in which prices rise well above fundamental values. Identifying bubbles and predicting crashes from price data alone is a notoriously difficult problem (1). However, prices are created by the collective behavior of the market participants, so neural activity could offer biomarkers for the evolution of price bubbles. Studies of asset price bubbles indicate a role for psychological factors such as "euphoria" (2), "irrational exuberance" (3), "mania" (4), "animal spirits" (5), and "sentiment" (6). We sought neural data supporting such psychological constructs that might help to identify price bubbles.

We observed the formation and crash of endogenous bubbles in experimental asset markets (7, 8) using multisubject neuroimaging. In each of 16 market sessions, consisting of an average of 20 traders (range, 11–23), we measured the neural activity of 2–3 participants (n = 44 total) using functional magnetic resonance imaging (fMRI). Our market design is based upon ref. 9. Traders could buy or sell one risky asset unit in each period. Fig. 1*A* illustrates the sequence of experimental events. Each market had 50 trading periods. All subjects began with 100 units of experimental currency (a risk-free asset) and 6 units of a risky asset. Each period, the risky asset paid a currency dividend d of either 0.40 or 1.00 per unit (with equal probability), creating an expected dividend $E[d]$ = 0.70. Currency earned a fixed interest rate r of 5% each period. After all 50 rounds of trading were completed, the risky asset was redeemed for 14 units of the risk-free currency.

These parameters defined an unambiguous fundamental value for the risky asset. Buying the risky asset in period t at price P_t and selling it one period later leads to the expected net gain $E_t[P_{t+1}]-P_t + E[d]$. The same investment of P_t in the risk-free asset yields a sure net gain of rP_t. If these two amounts are equal—in economic terms, if asset prices are "in equilibrium"—then there is a stationary price equal to a constant fundamental value F defined by $F=E[d]/r=0.70/0.05=14$. Prices persistently above F = 14 indicate a bubble; such a clear bubble measure is rarely available in field data. Fig. 2*A* illustrates the price paths for all 16 markets in this experiment. Bubbles are typical and large: the median price peak was 64.30 (range, 19.68–156.01). The bubble paths always result in a crash, and prices in the final period are near the fundamental F = 14 (median, 14.13). Fig. 2*B* illustrates a typical experimental session. This market bubble crashed after period 30. Trading volume is substantial, which means that prices do not result from a few extreme traders.

Results

A key computation during the asset market experiment involves the monitoring of round-to-round trading activity. Using a general linear model (GLM) of the blood oxygenation level-dependent (BOLD) signal of neural activity, we first established that the ventral striatum, including the nucleus accumbens (NAcc), responds strongly to both buying and selling outcomes revealed at the "Trading Results" screen (Fig. 3*A* and *SI Appendix*,

Significance

Asset price bubbles are an important example of human group decision making gone awry, but the behavioral and neural underpinnings of bubble dynamics remain mysterious. In multisubject markets determined by 11–23 subjects, with 2–3 subjects simultaneously scanned using functional MRI, we show how behavior and brain activity interact during bubbles. Nucleus accumbens (NAcc) activity tracks the price bubble and predicts future price changes. Traders who buy more aggressively based on NAcc signals earn less. High-earning traders have early warning signals in the anterior insular cortex before prices reach a peak, and sell coincidently with that signal, precipitating the crash. These experiments could help understand other cases in which human groups badly miscompute the value of actions or events.

Author contributions: A.S., T.L., P.R.M., and C.F.C. designed research; A.S. and J.K. performed research; A.S., T.L., and P.R.M. contributed new reagents/analytic tools; A.S. analyzed data; and A.S., T.L., P.R.M., and C.F.C. wrote the paper.

The authors declare no conflict of interest.

This article is a PNAS Direct Submission.

Freely available online through the PNAS open access option.

[1]To whom correspondence may be addressed. E-mail: acs@hss.caltech.edu, camerer@hss.caltech.edu, or read@vt.edu.

This article contains supporting information online at www.pnas.org/lookup/suppl/doi:10.1073/pnas.1318416111/-/DCSupplemental.

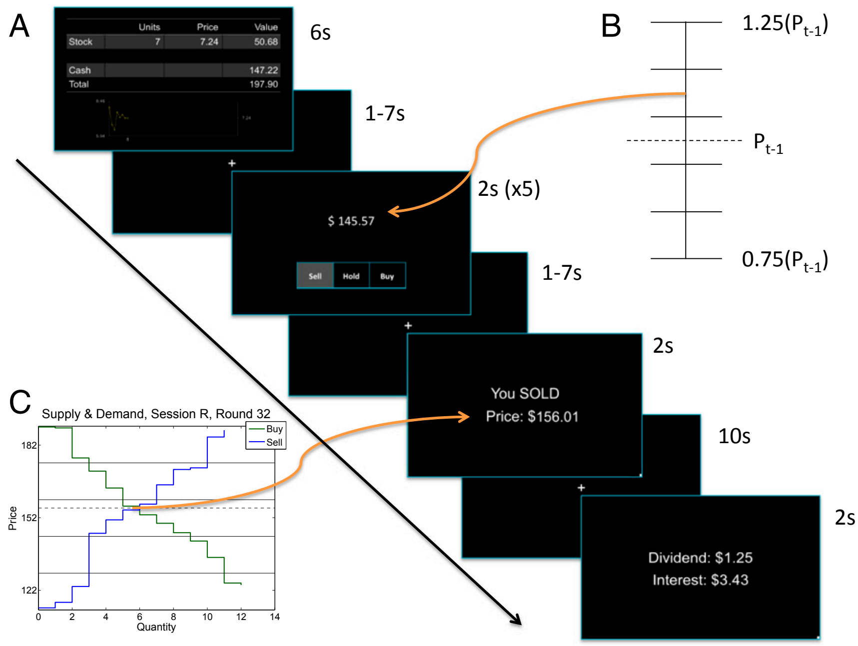

Fig. 1. Asset market experiment. (*A*) Each period subjects viewed the following screens, in order: Positions, Order Entry (×5), Trading Results, and Dividends and Interest. (*B*) Order elicitation procedure. Subjects responded Buy, Sell, or Hold to a random (uniform) price draw from each of five bins, each of width equal to 10% of the last period's price. The middle bin was centered on the last period's price. (*C*) How the price is chosen (=market clearing). The highest price at which subjects responded Buy, and the lowest price at which subjects responded Sell, were entered into a closed book call market. Prices and trading outcomes were reported on the Trading Results screen.

Table S4). In the call market mechanism that we use, subjects trade only when the market clearing price is below their expressed maximum willingness to buy (best bid), or is above their expressed minimum willingness to sell (best offer). Because the market price is unknown when the orders are placed, any trade therefore results in a positive reward prediction error. The NAcc receives a high density of projections from midbrain dopamine neurons, which are known to encode reward prediction error signals (10). Therefore, these GLM results are consistent with hundreds of studies that indicate that the NAcc plays a central role in the encoding of reinforcement, subjective value, and reward (11–13) (*SI Appendix*, Fig. S2*B*).

To connect the temporal dynamics of neural activity to the valuation dynamics reflected in the market price, we extracted trial-to-trial BOLD signal responses to the "Trading Results" screen (which shows both prices and bought-or-sold information) in a region of interest (ROI) centered on the bilateral NAcc [Montreal Neurological Institute (MNI) [±12, 8, −8]; see *SI Appendix*, Fig. S2*A*]. Recent studies have suggested a role for the NAcc in the evaluation of both states and policies (14), and we hypothesized that the time series of neural activity in the NAcc would contain information about the current state of the market (15). To test this hypothesis, we realigned neural and behavioral data from all of the sessions on a common timescale with 0 marking the peak price in each session. We then averaged the BOLD signal in our NAcc ROI across all subjects and then computed the moving average of the previous five periods of aggregate NAcc activity. The resulting moving-average NAcc time series is associated with the current level of the endogenous price bubble (Fig. 3*B*).

We next investigated whether neural activity in the NAcc could signal future price changes within a given market session. To do so, we calculated the five-period moving-average NAcc signal (as described above) within each session, and sorted this measure into three terciles. For each tercile of our market-level measure of NAcc activity, we computed the mean of the five-period forward return, $(p_{t+5} - p_t)/p_t$. Fig. 3*C* shows a clear and statistically significant difference between forward returns in the lowest tercile and forward returns in the highest tercile, with high values of NAcc activity associated with the lowest returns ($P < 0.001$, Mann–Whitney/Wilcoxon rank sum test for equality of distributions). Furthermore, Fig. 3*D* shows that when the within-session NAcc moving average is high, the empirical probability of a crash (defined as a drop of more than 50% in price over the next five trading rounds) is more than four times greater than when it is low (0.117 vs. 0.026; baseline, 0.075; $P < 0.001$, Fisher's exact test). Within the context of these experiments, neural activity in the NAcc appears to predict future changes in the price of the risky asset. Lower levels of NAcc activity are associated with higher future returns and low likelihood of a crash, whereas higher levels of NAcc activity are associated with low future returns and increased likelihood of a crash.

Many finance theories of bubbles describe mixtures of naïve backward-looking "momentum" investors, fundamental traders, and sophisticated investors who plan ahead (16–18). When bubbles form and crash, these three types will have low, medium, and high earnings, respectively. To investigate the relationship between individual task performance and neural activity, we sorted all subjects into three terciles of experimental earnings. These groups clearly have different patterns of dynamic share trading (Fig. 4*A*). However, Fig. 4*B* shows that the moving-average NAcc time series in the highest and lowest-earning groups are similar across trading periods.

Because average NAcc signal dynamics are similar in these two groups, but earnings performances are so different, we looked for an association across individuals between their NAcc-buying sensitivity and performance. For each trader, we computed $(\partial/\partial N_t)p(B_{t+1})$ via logistic regression, where $p(B_{t+1})$ is the probability of buying at time $t + 1$ and N_t is the average NAcc activity at time t over the five periods from $t - 4$ to t. The partial derivative $(\partial p(B_{t+1}))/\partial N_t$ is a brain-buying signal: it measures the change in propensity to buy as a function of recent NAcc activity.

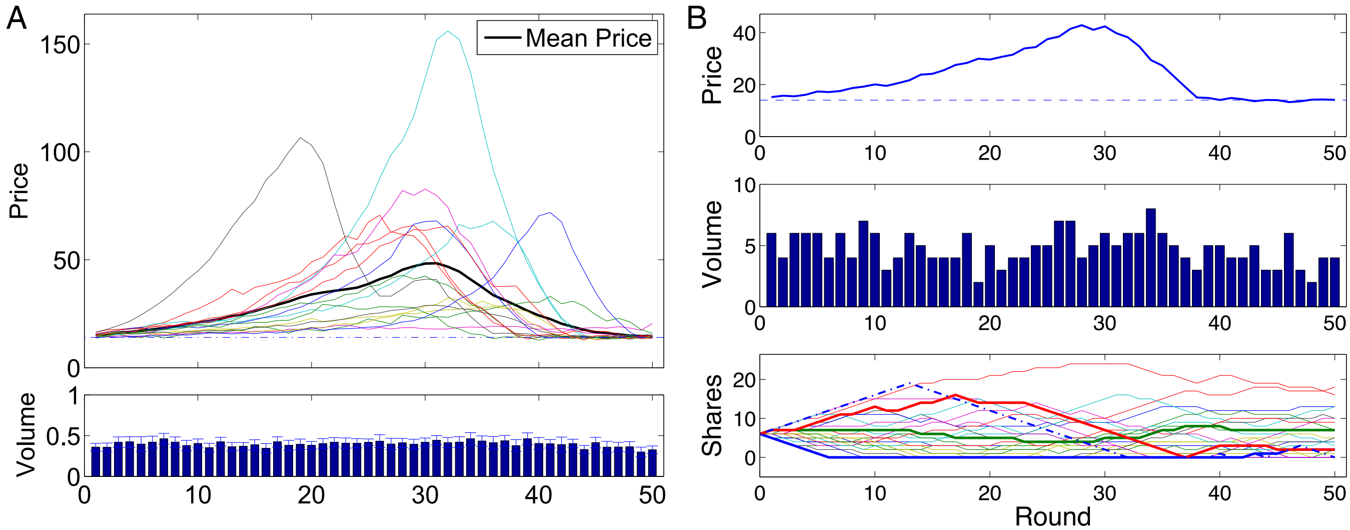

Fig. 2. Endogenous market bubbles. (*A*) Price paths in16 different experimental market sessions. The dark line shows the average price in each period over the 16 sessions. Plotted below the prices is the normalized per-subject volume for each period; error bars are SEs. (*B*) Single-session prices (*Top*) and trading volume (*Middle*) from one statistically typical experimental session. At *Bottom* is shown the risky asset holdings; each subject is indicated by a different color. MRI subjects are shown with thicker lines. The dashed line is the "clairvoyant" profit-maximizing share path (assuming subjects could somehow correctly anticipate all future prices).

Fig. 4*C* plots individual trader profits against $(\partial p(B_{t+1}))/\partial N_t$. The relation is significantly negative ($\rho = -0.52$, $P < 0.001$). The negative slope measures the economic cost of "following one's nucleus accumbens."

We also used interval regression analysis to estimate the independent contribution of neural activity in several ROIs to future valuation (*SI Appendix*). We find that the NAcc response is positively associated with demand for the risky asset in subsequent trading periods, after controlling for observable variables such as returns, dividend yield, and the individual's current policy (*SI Appendix*, Table S7). This pattern appears to be driven by a stronger brain–behavior link in low-earning subjects.

Although low earners are net buyers around the price peak, high earners begin to sell their shares a few periods before the

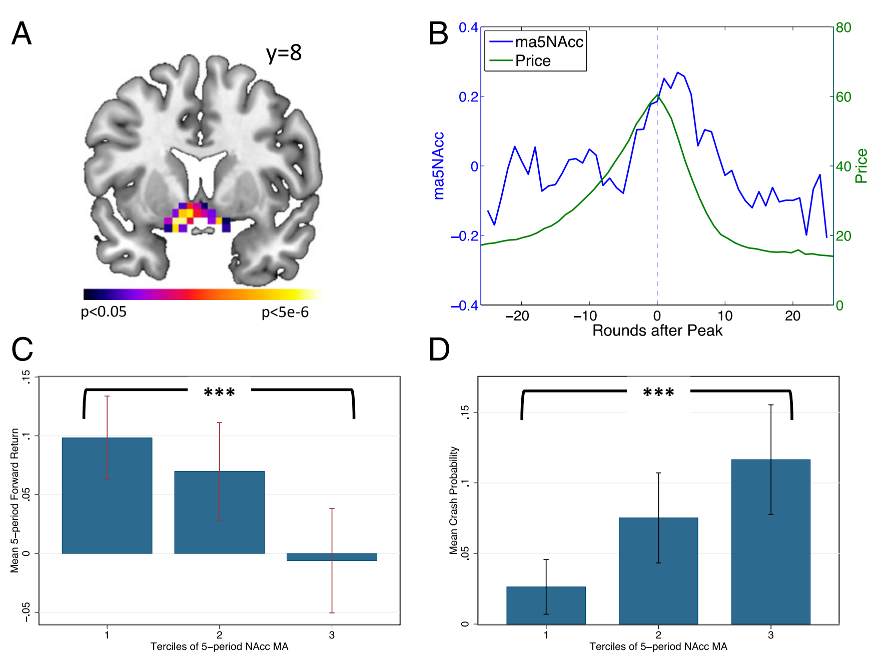

Fig. 3. Irrational exuberance. (*A*) GLM results showing the conjunction of neural responses to "You Bought" and "You Sold" messages; $P < 0.05$ (familywise error corrected). Peak T = 7.69, MNI = [−10, 8, −14]. (*B*) Average NAcc activity tracks the endogenous market bubble. MA5Nacc (blue) is the average of the five previous periods' NAcc activity, recentered around the maximal (peak) price in each session. (*C*) NAcc activity predicts future returns of the risky asset. Earners were divided into three groups, by terciles of earnings. Each bar shows the mean five-period forward return, for each tercile of the five-period moving average of NAcc activity, calculated within session. The mean return in the highest tercile of NAcc activity is significantly less than the mean return in the lowest tercile. (*D*) NAcc activity within session predicts crashes. Each bar shows the relative frequency of a crash (defined as a price drop of greater than 50%) occurring in the next five periods. The observed incidence of crashes is much greater in the highest tercile of our moving-average NAcc activity signal.

bubble peak (Fig. 4*A*). To investigate the neural activity associated with the switch to selling before the peak, we focused a priori on the anterior insular cortex. The insula is an "interoceptive" area that is active during bodily discomfort and unpleasant emotional states, such as pain, anxiety, and disgust. Its anterior region is thought to be associated with the awareness of bodily states (19, 20). Anterior insula is also activated by financial risk (21, 22) and by variance in prediction errors, a measure of uncertainty in temporal-difference learning models (23). We hypothesized that neural activity in the anterior insula might motivate sophisticated participants to begin selling the risky asset. Fig. 4*D* shows the average BOLD activity paths from the anterior insular cortices of the high- and low-earnings groups (using an ROI centered at MNI [36, 24, 2], radius of 6 mm, based on ref. 21; *SI Appendix*, Fig. S3). Near the time that the two groups begin their respective shifts to selling and buying, insula activity increases in the high earners but there is no similar response in the low earners.

Analogously to the previous NAcc-buying sensitivity analysis, we measured the association between the insula-selling relationship and performance. Fig. 4*E* plots total earnings against $(\partial p(S_{t+1}))/\partial I_t$, where $p(S_{t+1})$ is the probability of selling at time $t + 1$, and I_t is the average neural activity in the right anterior insula at time t over the previous five periods (including time t). This measure of the neural brain-selling link is positively correlated with performance ($\rho = 0.46$, $P < 0.003$). In the high earners, the right anterior insula signal seems to encode a risk detection or warning signal that is associated with selling profitably.

Discussion

The experimental method is ideal for understanding the neuropsychology of asset bubbles, because the experimenter can control the fundamental asset value, and hence clearly identify when prices are too high (1–3, 18, 24, 25). Our experimental design used live trading to show that asset price bubbles result endogenously from interactions between different types of traders. Traders react to buy or sell events and represent bubble magnitude commonly in the NAcc [also observed in other investment decision tasks (26–28)]. Elevated NAcc activity is associated with low future returns and higher likelihood of a crash. Therefore, NAcc activity in our experiments appears to provide an indicator for price bubbles that is consistent with historical accounts of euphoria and irrational exuberance near the peak in prices.

Traders who buy more aggressively given NAcc signals perform worse in the task. The slope of this buy/NAcc relation represents a new "neurobehavioral metric" for the financial cost of "irrational exuberance" and could be used as quantitative and parametric biomarker in other contexts where humans overvalue

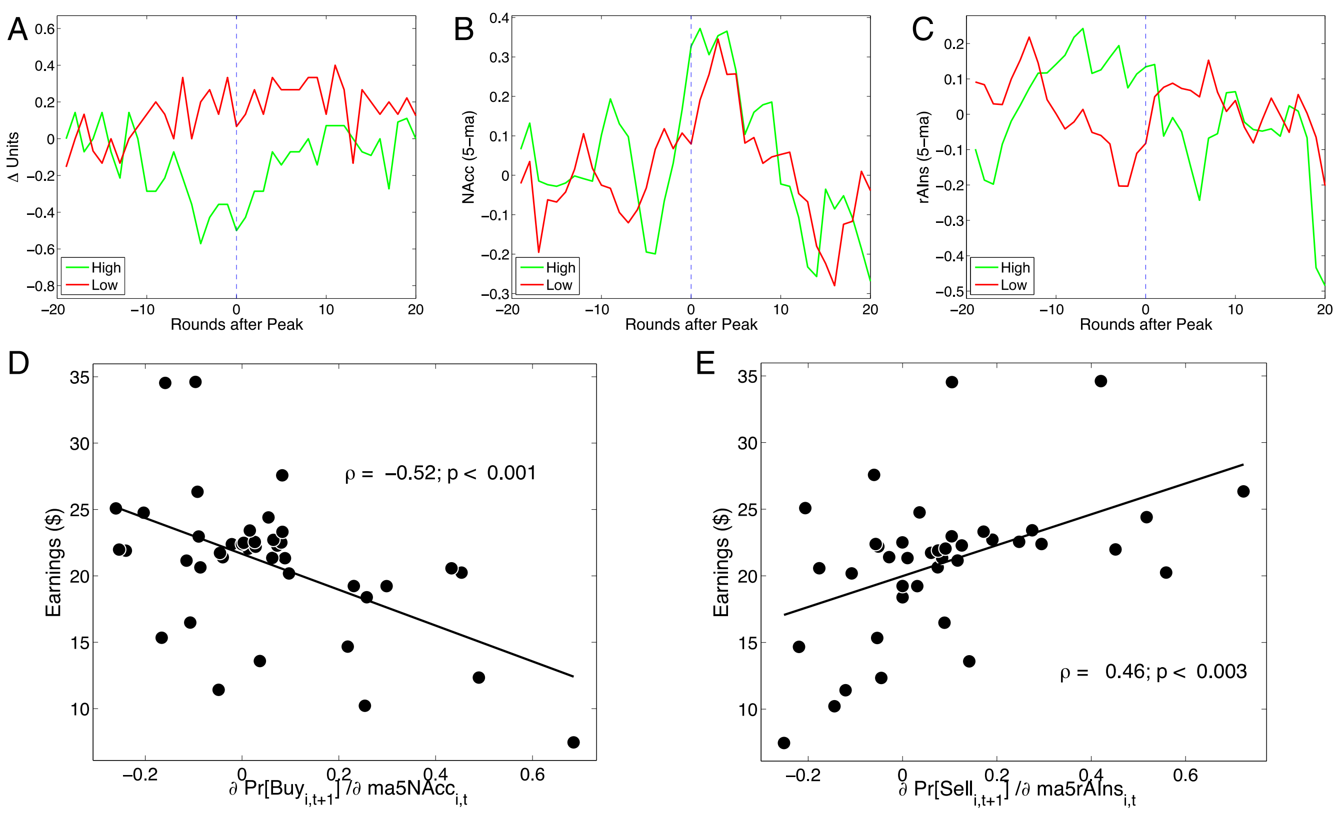

Fig. 4. Individual differences: high and low earners and neurobehavioral metrics. (*A*) Trading behavior of the highest and lowest earnings terciles, aligned around the market peaks. The *y* axis plots the mean change in units of the risky asset in each period. These trading curves cross about 10 periods before the peak of the market. The high earners' sell-off continues unabated until about 10 periods after the peak. (*B*) The NAcc activity association of prices appears to be consistent across subject groups. The colored lines plot the mean NAcc activity in the highest and lowest terciles of the payout distribution. (*C*) Average right anterior insula activity in high earners and low earners shows that low earner activity fluctuates around 0, whereas high earner activity shows a peak that coincides with the beginning of the sell-off of units shown in *A* (5–10 periods before the price peak). We used an ROI centered on MNI [36, 24, 2], corresponding to the peak "risk prediction" signal from ref. 23. (*D*) The cost of changing one's buying probability as a function of the change in activity in the NAcc as read out by earnings. Forty-one scanned subjects are included in this plot. The negative slope shows that tracking the group-defined bubble and committing to it in the form of increased brain-to-buying probability costs money. This defines a neural metric for irrational exuberance and measures it in terms of earnings. (*E*) Increased propensity to sell based on right anterior insula activity (a neurobehavioral brain-selling relation) is associated with higher earnings. The positive slope shows that subjects whose insula activity is predictive of future selling earn more.

bad acts or outcomes like compulsive gambling, overeating, or drug addiction (29).

Another neurobehavioral finding is a positive association between trading performance and selling when neural activity in the anterior insula is elevated. The insula signal may reflect increased perception of risk (21–23) or of uncomfortable bodily states (19, 20). The presence of an elevated insula signal in the high earners before the price peak, its concurrent absence in the low earners, its association with trading pattern changes, and the stronger neurobehavioral insula-selling link among high earners suggest that increased neural activity in the right anterior insula may constitute an early warning signal for these individuals to begin switching from the risky to the risk-free asset. The evidence from both of our neurobehavioral metrics is consistent with the study by Kuhnen and Knutson (26), who show that activations in both of these regions can lead to shifts in risk preferences.

Many theories of bubbles in large natural markets depend on economic agents' incentives (30) or on market structure (31). A recent literature examines the interaction between valuation and media coverage (32–34). Another explanation involves traders who get internal signals (or "hunches") that a bubble exists; bubbles then persist because traders who get early signals keep buying, expecting that the other traders' signals will not arrive until later (35). However, these theories do not specify neural mechanisms (36). Our evidence is consistent with bubble accounts based on bounded rationality, emotion, and neural activity (2–9, 16–18, 36, 37). Warren Buffet famously said, "Be fearful when others are greedy, and greedy when others are fearful." Our experimental results support the first part of his advice to a surprising degree: Wiser traders who begin selling when their insula is active (indicating discomfort) sell a few periods before the peak to traders with the highest "greed," measured by increased NAcc-buying sensitivity.

Our results contribute to understanding the biological basis of group valuation in natural asset markets. Modern examples of bubbles in the last three decades include stocks in Japan, in China, and in the US high-tech sector, and housing in many countries. Bubbles redistribute enormous wealth and can leave long-lasting macroeconomic scars, and are therefore important to both investors and policymakers. In 1996, Federal Reserve Chair Alan Greenspan asked: "But how do we know when irrational exuberance has unduly escalated asset values?" (38). His successor, Ben Bernanke, suggested "progress will require careful empirical research with attention to psychological as well as economic factors" (39). Our results point in the direction of theories based on an interaction between traders with exuberant valuation and forward-looking traders who ride bubbles, and then sell when they feel uncertain.

Materials and Methods

We conducted 16 experiment sessions (2 in October 2011, 8 in January 2012, and 6 in April 2012) with 320 total subjects. Each session included between 11 and 23 subjects (mean, 20; min, 11; max, 23). The majority of our subjects (276 total) were University of California, Los Angeles, students participating in the experiment at the California Social Science Experimental Laboratory (CASSEL). In addition, 2–3 individuals per session (44 total) took part in the experiment from two locations at the Virginia Tech Carilion Research Institute (Blacksburg and Roanoke, VA). These subjects underwent fMRI of their neural activity during the experiment. All participants were networked together via a special experiment software package, NEMO, to conduct the experiment. NEMO was designed for use with multiple subjects in the scanner.

Of the 44 total subjects we scanned, 2 subjects were dropped because of technical issues with syncing behavioral and functional imaging data. One additional subject was dropped because the subject had no "Sell" transactions, leaving 41 fMRI subjects.

Behavior-only participants received a $5 show-up payment, whereas subjects who underwent fMRI scanning received an additional payment of $50. Before trading began, the experimenters read the instructions aloud. Subjects then took a five-question quiz (reproduced below), after which the experimenters reviewed the quiz answers. In addition, subjects participated in three practice trading rounds before live trading began.

SI Appendix, Table S1, provides summary statistics separately for subjects who did and did not undergo imaging. We also conducted one pilot session where all subjects (behavior-only and fMRI) were located in Virginia; this session is included in the data. Our scanned subjects are in general older (mean age, 28.43 vs. 23.15). In addition, 85% of our scanned population indicated their race as White or Hispanic, whereas 70% of our behavior-only subjects indicated that their race was Asian. The sex balance for both groups is close to 50%.

ACKNOWLEDGMENTS. We thank Nathan Apple for help implementing the large group experiment across three cities and four sites simultaneously. We also thank Antonio Rangel for contributions to the early stages of this project. This research was supported by National Science Foundation Grant SES-00-99209, the Gordon and Betty Moore Foundation, the Lipper Family Foundation (C.F.C.), National Institutes of Health Grants DA11723 and MH085496 (to P.R.M.), The Kane Family Foundation (P.R.M.), Defense Advanced Research Projects Agency (P.R.M.), and a Wellcome Trust Principal Research Fellowship (to P.R.M.).

ECONOMIC SCIENCES

NEUROSCIENCE

1. Flood RP, Garber PM (1980) Market fundamentals versus price-level bubbles: The first tests. *J Polit Econ* 88(4):745–770.
2. Kindleberger CP, Aliber RZ (2005) *Manias, Panics, and Crashes: A History of Financial Crises* (Wiley, Hoboken, NJ).
3. Shiller R (2005) *Irrational Exuberance* (Broadway Books, New York), 2nd Ed.
4. Ofek E, Richardson M (2003) Dotcom mania: The rise and fall of internet stock prices. *J Finance* 58(3):1113–1138.
5. Akerlof G, Shiller R (2009) *Animal Spirits: How Human Psychology Drives the Economy, and Why It Matters for Global Capitalism* (Princeton Univ Press, Princeton).
6. Baker M, Wurgler J (2006) Investor sentiment and the cross-section of stock returns. *J Finance* 61(4):1645–1680.
7. Plott CR, Sunder S (1988) Rational expectations and the aggregation of diverse information in laboratory security markets. *Econometrica* 56(5):1085–1118.
8. Smith VL, Suchanek GL, Williams AW (1988) Bubbles, crashes, and endogenous expectations in experimental spot asset markets. *Econometrica* 56(5):1119–1151.
9. Bostian AJ, Holt CA (2009) Price bubbles with discounting: A Web-based classroom experiment. *J Econ Educ* 40(1):27–37.
10. Montague PR, Dayan P, Sejnowski TJ (1996) A framework for mesencephalic dopamine systems based on predictive Hebbian learning. *J Neurosci* 16(5):1936–1947.
11. Montague PR, Hyman SE, Cohen JD (2004) Computational roles for dopamine in behavioural control. *Nature* 431(7010):760–767.
12. Yarkoni T, Poldrack RA, Nichols TE, Van Essen DC, Wager TD (2011) Large-scale automated synthesis of human functional neuroimaging data. *Nat Methods* 8(8):665–670.
13. Bartra O, McGuire JT, Kable JW (2013) The valuation system: A coordinate-based meta-analysis of BOLD fMRI experiments examining neural correlates of subjective value. *Neuroimage* 76:412–427.
14. Li J, Daw ND (2011) Signals in human striatum are appropriate for policy update rather than value prediction. *J Neurosci* 31(14):5504–5511.
15. Kishida KT, et al. (2011) Sub-second dopamine detection in human striatum. *PLoS One* 6(8):e23291.
16. Shleifer A (2000) *Inefficient Markets* (Oxford Univ Press, Oxford).
17. Barberis N, Greenwood R, Jin L, Shleifer A (2013) X-CAPM: An extrapolative capital asset pricing model. *NBER Working Paper* (National Bureau of Economic Research, Cambridge, MA), No. 19189.
18. Haruvy E, Noussair CN (2006) The effect of short selling on bubbles and crashes in experimental spot asset markets. *J Finance* 61(3):1119–1157.
19. Critchley HD, Wiens S, Rotshtein P, Öhman A, Dolan RJ (2004) Neural systems supporting interoceptive awareness. *Nat Neurosci* 7(2):189–195.
20. Craig AD (2009) How do you feel—now? The anterior insula and human awareness. *Nat Rev Neurosci* 10(1):59–70.
21. Preuschoff K, Bossaerts P, Quartz SR (2006) Neural differentiation of expected reward and risk in human subcortical structures. *Neuron* 51(3):381–390.
22. Mohr PN, Biele G, Heekeren HR (2010) Neural processing of risk. *J Neurosci* 30(19): 6613–6619.
23. Preuschoff K, Quartz SR, Bossaerts P (2008) Human insula activation reflects risk prediction errors as well as risk. *J Neurosci* 28(11):2745–2752.
24. Camerer C, Weigelt K (1993) *Double Auction Markets*, eds Friedman D, Rust J (Addison-Wesley, Redwood City, CA).
25. Dufwenberg M, Lindqvist T, Moore E (2005) Bubbles and experience: An experiment. *Am Econ Rev* 95(5):1731–1737.
26. Kuhnen CM, Knutson B (2005) The neural basis of financial risk taking. *Neuron* 47(5): 763–770.
27. Lohrenz T, McCabe K, Camerer CF, Montague PR (2007) Neural signature of fictive learning signals in a sequential investment task. *Proc Natl Acad Sci USA* 104(22): 9493–9498.
28. De Martino B, O'Doherty JP, Ray D, Bossaerts P, Camerer C (2013) In the mind of the market: Theory of mind biases value computation during financial bubbles. *Neuron* 79(6):1222–1231.
29. Brewer JA, Potenza MN (2008) The neurobiology and genetics of impulse control disorders: Relationships to drug addictions. *Biochem Pharmacol* 75(1):63–75.

30. Allen F, Gorton G (1993) Churning bubbles. *Rev Econ Stud* 60(4):813–836.
31. Hong H, Scheinkman J, Xiong W (2006) Asset float and speculative bubbles. *J Finance* 61:1073–1117.
32. Dyck A, Zingales L (2003) The bubble and the media. *Corporate Governance and Capital Flows in a Global Economy*, eds Cornelius P, Kogut B (Oxford Univ Press, Oxford, UK).
33. Veldkamp L (2006) Media frenzies in markets for financial information. *Am Econ Rev* 96(3):577–601.
34. Bhattacharya U, Galpin N, Ray R, Yu X (2009) The role of the media in the Internet IPO bubble. *J Financ Quant Anal* 44(3):657–682.
35. Abreu D, Brunnermeier M (2003) Bubbles and crashes. *Econometrica* 71(1):173–204.
36. Lo A (2013) Fear, greed, and financial crises: A cognitive neurosciences perspective. *Handbook on Systemic Risk*, eds Fouque JP, Langsam J (Cambridge Univ Press, Cambridge, UK).
37. Shefrin H (1999) *Beyond Greed and Fear* (Oxford Univ Press, Oxford, UK).
38. Greenspan A (1996) The Challenge of Central Banking in a Democratic Society. Available at www.federalreserve.gov/boarddocs/speeches/1996/19961205.htm. Accessed June 12, 2014.
39. Bernanke B (2010) Implications of the Financial Crisis for Economics. Available at www.federalreserve.gov/newsevents/speech/bernanke20100924a.htm. Accessed June 12, 2014.

Supporting Information

Irrational exuberance and neural crash warning signals during endogenous experimental price bubbles

Alec Smith[1], Terry Lohrenz[2], Justin King[2], P. Read Montague[2,3], Colin F. Camerer[1]

1. California Institute of Technology, Pasadena, CA
2. Virginia Tech Carilion Research Institute, Roanoke, VA
3. The Wellcome Trust Centre for Neuroimaging, University College London, UK

Behavioral Results

Market statistics. Table S1 reports summary price and volume statistics at the aggregate and session levels. To enable comparisons with other studies of laboratory asset bubbles we also report summary statistics that measure the extent of deviations from fundamental value: the Relative Absolute Deviation and Relative Deviation for each session.(*1*) Both measures are volume weighted, so that they take into account the number of trades at a given price. Relative Absolute Deviation (RAD) is computed as

$$RAD = \frac{\sum_{t=1}^{50} v_t \left(\frac{|p_t - 14|}{14}\right)}{\sum_{t=1}^{50} v_t}$$

and Relative Deviation (RD) is computed as

$$RD = \frac{\sum_{t=1}^{50} v_t \left(\frac{p_t - 14}{14}\right)}{\sum_{t=1}^{50} v_t}$$

where p_t is the price in each round t and v_t is the number of units traded in each round. RAD is a measure of “mispricing”: an RAD of 0.1 means that the average trade takes place at a price that is 10% different from than fundamental value. RD adds directional measures: an RD of 0.1 means that the average trade takes place at a price that is 10% greater than fundamental value. In our experiments, the mean RAD is 1.050 and the mean RD is 1.047, indicating that the average trade takes place at 104.7% of fundamental value. The mean RAD and mean RD are very close in magnitude because in almost all rounds, the price is greater than fundamental value. For comparison, in the experiments reported by (*2*), the largest reported RAD is 0.414 and the largest observed RD is 0.297, so our experiments produce bubbles of magnitude roughly three times as large.

Scanned vs. behavioral participants. Behavioral participants scored slightly higher on the pre-experiment quiz (Table S1: mean score 3.87 vs. 3.43 for the scanned participants), and this difference is significantly different from 0 at the 5% level using a two-sided t-test for difference in means (n =317, p-value 0.04). However, this difference in quiz performance did not appear to result in a noticeable difference in trading behavior or performance. Figure S2 compares trading activity and payout for the experiment for our two subject populations. This comparison is important because undergoing neuroimaging might affect behavior, so that the behavior of our scanned population might be different in some way from the population of non-scanned behavioral subjects. On average, subjects traded in 19.31 rounds (std. dev. 9.19, range 2-44). The mean payout in the experiment was $20.86 (std. dev. 5.27, range 4.07-45.62). There are no significant differences between the two groups in either the number of trades (p=0.339, Wilcoxon rank-sum test; p = 0.3223, Kolmogorov-Smirnov test) or in payouts (p = 0.2164, Wilcoxon rank-sum test; p = 0.1551, Kolmogorov-Smirnov test).

Individual characteristics associated with trading behavior and performance. We used multiple regression analysis to explore whether demographic factors were associated with trading behavior and performance. Table S3 reports the results from ordinary least squares regressions of: (Model 1) payout on demographic variables and quiz scores; (Model 2) Number of trades on demographic variables and quiz scores; (Model 3) Quiz score on demographic variables. The results from Model 1 suggest that the main subject-level variable that influences payouts are task comprehension and trading activity: scoring one additional question right on the pre-experiment quiz is associated with earning an additional $0.75. On average trading is costly: each additional trade results in an average loss of $0.14. Note however that the relationship of trades to payouts is nonlinear: the very highest earners (roughly, the highest 20%) trade more than average, as do the lowest earners. Furthermore, any subject can guarantee himself or herself the mean payout in a given session by not trading at all. Cancelled trades, potentially a measure of subject confusion, had a negative but statistically insignificant association with payout. Model 2 suggests that Asian subjects make on average almost 4 more trades than Black or White subjects; and Model 3 shows that on average male subjects score on average almost ½ point higher on the pre-experiment quiz relative to female subjects.

Imaging Protocol

Image acquisition and analysis. The imaging was conducted on three 3.0T Siemens Magentom Trio scanners at the Virginia Tech Carilion Research Institute. Two scanners are located in Roanoke, VA and one in Blacksburg, VA. Two separate cohorts of imaging data were collected for this experiment: one in October 2011 and January 2012, and another in April 2012. The first cohort comprised of 27 healthy subjects recruited in accordance with a protocol approved by the Virginia Tech Institutional Review Board. High-resolution T1-weighted scans were acquired using a magnetization prepared rapid gradient echo sequence. Functional imaging were acquired with a repetition time of 2000 ms and an echo time of 30 ms. Twenty-six 4-mm slices were acquired parallel with the anteroposterior commissural line, yielding functional voxels that were 3.4mm x 3.4mm x 4mm. The second cohort of 17 healthy subjects were recruited in the same method and matched the parameters of the high-resolution scans from the initial cohort. Functional images from cohort two were acquired with a repetition time of 2000 ms and an echo time of 25 ms. Thirty-seven 4-mm slices were acquired 30° off the anteroposterior commissural line, yielding functional voxels that were 3.4mm x 3.4mm x 4mm.

Image preprocessing. Images were analyzed using SPM8 (http://www.fil.ion.ucl.ac.uk/spm/software/spm8/). Slice timing correction was first applied to temporally align all the images. Motion correction to the first functional image was performed using a six-parameter rigid-body transformation. Images were subsequently spatially normalized to the Montreal Neurological Institute template by applying a 12-parameter affine transformation, followed by nonlinear warping using standard basis functions. Finally, for GLM analyses, the images were smoothed with an 8 mm isotropic Gaussian kernel and then high-pass filtered (128 s width) in the temporal domain.

Imaging Analyses

General linear model. We initially estimated the following general linear model (GLM) of BOLD responses with an AR(1) structure. In each voxel we regressed the preprocessed, spatially smoothed BOLD signal on (1) Indicators for each each of the four different stimulus screens (Positions, Order Entry, Trading Results, and Dividends and Interest); (2) Separate indicators for trials where subjects bought and sold (i.e., trials where subjects saw "You Bought" or "You Sold" messages); (3) Parametric regressors for the expected dividend yield and the return at the time outcomes are revealed (the "Trading Results" screen). The expected dividend yield in round t is $\mathrm{E}[d_t]/p_t = 0.7/p_t$. Return is defined as $(p_t - p_{t-1})/p_{t-1}$: the fractional change in price from the previous round. All regressors of interest are convolved with a canonical hemodynamic response function (Friston et al., 1998). We also included the time series of 6 head motion parameters estimated from preprocessing as a regressor of no interest, to control for residual head motion in the time series.

Imaging results. An overview of the results from this analysis is given in Table S4. We found strong responses to "You Bought" and "You Sold" messages in the ventral striatum, relative to our baseline of "No Trade" messages (both results are significant at the 5% level, after adjusting significance levels for multiple comparisons across the whole brain using Family Wise Error (FWE) corrections). We found few differences in neural responses to "Buy" and "Sell" messages, even at much more liberal significance thresholds (p-value 0.005, uncorrected), save a small cluster in the middle frontal gyrus for the contrast "Bought"-"Sold".

We also found that neural activity responded negatively to expected dividend in the ventral striatum and subgenual cingulate cortex. This result is consistent with the analysis in the main text; the expected dividend is the inverse of the price, times a constant. In addition we found neural activity in a number of brain regions associated with theory-of-mind tasks, such as the superior temporal gyrus. We found few neural correlates of return except at very liberal thresholds, where we note a small cluster in the superior temporal gyrus, in a region where neural activity is often associated with theory-of-mind tasks.

Trial to trial data extraction. We extracted the trial-to-trial data as follows: After preprocessing (see above), we filtered the (unsmoothed) time course of BOLD responses in each voxel using a high-pass filter with bandwidth 128s. We then removed any remaining linear trend by regressing the filtered time course in each voxel on a constant and linear time trend and extracting the residuals. Next, we estimated the baseline BOLD responses to each of the four different stimulus screens (Positions, Order Entry, Trading Results, and Dividends and Interest), using a GLM of the BOLD responses with an AR(1) serial correlation structure. The model included regressors for each of the four screens, each convolved with a canonical hemodynamic response function (*3*), as well as the time series of 6 head motion parameters estimated from preprocessing. This model estimates neural responses that are associated with a given stimulus, but not the neural computations that are involved in assessing the stimulus. The (whitened) residuals from this regression capture trial-to-trial variation in BOLD responses.

The next step was to compute, for each subject and each voxel, the neural response to each of the 50 "Trading Results" screens. We approximated the peak hemodynamic response by interpolating between the two volumes acquired closest to 5 seconds after the stimulus onset. The result is a (50 x approximately 25,000 voxels) matrix of data containing the residual variation in BOLD responses to new trading and price information. From this we can examine the trial-to-trial responses in any region of interest. To facilitate cross-subject comparison, we normalized the response in each voxel to have mean 0 and standard deviation 1, then averaged the normalized responses in each region of interest (e.g. the NAcc).

Regions of interest. For the bilateral NAcc region of interest (ROI), we used an anatomical mask consisting of a 6mm-radius sphere centered on MNI coordinates (±12,8,-8). The resulting mask is shown in Figure S2 (Panel A) and contains a total of 24 voxels. This ROI contains the peak signal from the Neurosynth reverse-inference "reward" map (Figure S2B). The map shows regions that are more likely to be reported in studies that use the term "reward" frequently (329 studies of the 5089 in the Neurosynth database as of July 10, 2013) (*4*). The peak z-scores for this reverse-inference map are located at MNI (10,12,-10) (right NAcc) and (-10 , 10 ,-8) (left NAcc). Both locations are contained in our NAcc mask. We also list the top terms from the structure-to-function reverse inference feature map located at the center of our NAcc ROI in Table S5. The table shows terms that appear with high frequency from the 167 studies in the Neurosynth database that report activation within 6 mm of MNI coordinates (12,8,-8). Prominent features at this location include "reward", "incentives", and "feedback".

For the Anterior Insula ROI, we used a 6mm radius sphere, centered on MNI coordinates (36,24,2) located in the right Anterior Insula. These coordinates correspond to the peak "risk prediction" signal from (5), after converting from Talairach to MNI coordinates.

In the interval regressions below (Table S7) we employ as control variables neural activity at the time of the "Trading Results" screen extracted from ROIs in the Amygdala, left Dorsolateral Prefrontal Cortex (lDLPFC), and right Temporoparietal junction (rTPJ). The Amygdala ROI is based on an the Automated Anatomical Labeling (AAL) Amygdala mask (*6*). The lDLPFC mask is a 6mm-radius sphere centered at MNI (-40,44,18), and the rTPJ sphere is a 6mm-radius sphere centered at MNI (56,-56,16). We also employ an additional ROI, in the left Intraparietal Sulcus (lIPS) as a control region for our brain-behavior association analysis. The lIPS ROI is a 6mm-radius sphere centered on MNI (-31,-62,48).

Brain-Behavior Associations

The scatterplot in Figure 4D in the main text shows that buying when neural activity in the nucleus accumbens is high is associated with low overall profits in the experiment. Similarly, the scatterplot in Figure 4E shows that selling when neural activity is in the right anterior insula is high is associated with higher profits. For both of these analyses, the variable on the x-axis is determined by generating a dependent variable indicating whether the subject bought (or in Figure YY, sold) in round *t*, and then regressing this binary dependent variable on the 5-period moving average of neural activity in the given region of interest at round *t-1*. The x-axis plots the marginal effects from these regressions: the change in probability of buying (or selling) with respect to a 1 unit change in our measure of neural activity. The y-axis in these plots shows each subject's earnings for the experiment, in US dollars.

Figure S3B illustrates that we find no significant brain-buying relationship in the right anterior insula ROI. Figure S4 shows the results from the comparison of both brain-buying and brain-selling relationships with earnings in two additional regions-of-no-interest. Figures S4A and S4B show brain-trading relationships in the rTPJ. Figures S4C and S4D show brain-trading relationships in the lIPS. We selected the rTPJ for its association with theory-of-mind tasks (7), and the lIPS for its association with numerosity (8). We find no significant association between earnings and the neurobehavioral metrics (either brain-buying or brain-selling) from either the rTPJ or lIPS.

Table S6 shows linear regression analyses that illustrate relationships between the NAcc-buying and insula-selling metrics and earnings, with increasing numbers of control variables. Models 1 and 2 show simple linear regressions of earnings on the NAcc-buying association and the insula-selling association, respectively. Model 3 includes both measures and adds subject's score on the pre-experiment quiz. The NAcc-buying association and the insula-selling metrics are each independently statistically significantly associated with task performance. The model in column 4 shows that when increased neural activity in the NAcc is associated with subsequent buying, earnings are lower, and when increased neural activity in the insula is associated with subsequent selling, earnings are higher, after controlling for gender, race, and performance on the pre-experiment quiz.

Interval regression analyses

Model. Our order entry procedure elicits a demand curve for the risky asset, for each subject in each round. We use the elicited orders, namely the highest price to which a subject responds "Buy" and the lowest price to which a subject responds "Sell", to estimate the price at which a subject is indifferent between buying and selling (measured as a percentage of the last period's price).

The experiment protocol presented 5 randomly-ordered stimulus prices each trading round ($s_{it}^k, k \in \{1,2,3,4,5\}$). Subjects indicate whether they prefer to buy, hold, or sell if the price is s_{it}^k in round t. We assume that subject *i*'s demand curve $x_i(p_t)$ for the risky asset in round t is downward sloping in the price p_t. Given this assumption there is some price p_{it}^* such that $x_i(p_{it}^*) = 0$. At prices greater p_{it}^*, the subject prefers selling, while at prices lower than p_{it}^*, the subject prefers selling.

To study the determinants of demand for the risky asset, we let $y_{it}^* = (p_{it}^* - p_{t-1})/p_{t-1}$ and assume that $y_{it}^* \sim \mathrm{N}(Z_{it}\gamma, \sigma^2)$ and we estimate the coefficients γ via maximum likelihood. We normalize by the market price in the previous round because the price process, and also the response data, has a unit root. Thus our dependent variable is the price at which a subject is indifferent between buying and selling, expressed as a fraction of the previous round's price.

Define the categorical variable y_{it} as follows:

$$y_{it} = \begin{cases} -1 \; if \; p_{it}^* \le \min_k s_{it}^k \\ 0 \; if \; \min_k s_{it}^k < p_{it}^* \le \max_k s_{it}^k \\ 1 \; if \; \max_k s_{it}^k \le p_{it}^* \end{cases}$$

We define a_{it} as the highest stimulus price s_{it}^k/p_{t-1} to which subject i responds Buy, expressed as a fraction of the previous round's price; and similarly let b_{it} denote the lowest stimulus price s_{it}^k/p_{t-1} to which subject i responds Sell, again normalizing by the previous price; then y_{it}^* lies in the interval $[a_{it}, b_{it}]$ and $y_{it} = 0$. If we observe Buy responses but not Sell responses in round t, then $y_{it}^* \in [a_{it}, +\infty]$ and $y_{it} = 1$. Similarly if there are no Buy responses then $y_{it}^* \in [-\infty, b_{it}]$ and $y_{it} = -1$.

The log-likelihood function is

$$L(\gamma, \sigma) = \sum_{i=1}^{I} \sum_{t=1}^{50} \left\{ \begin{array}{l} 1[y_{it} = -1] \log\left(\Phi\left(\frac{b_{it} - Z_{it}\gamma}{\sigma}\right)\right) + \\ 1[y_{it} = 0] \log\left(\Phi\left(\frac{b_{it} - Z_{it}\gamma}{\sigma}\right) - \Phi\left(\frac{a_{it} - Z_{it}\gamma}{\sigma}\right)\right) + \\ 1[y_{it} = 1] \log\left(1 - \Phi\left(\frac{a_{it} - Z_{it}\gamma}{\sigma}\right)\right) \end{array} \right\}$$

where $1[\cdot]$ is the indicator function and $\Phi(\cdot)$ is the cumulative distribution function for the standard normal distribution. This approach is known as interval regression (cf. (9)).

Under more restrictive assumptions, we can motivate our regression model with respect to subject's beliefs about future returns. Assume that at time t subjects maximize the constant absolute risk aversion (CARA) utility function $u(W_{t+1}) = -e^{-\rho W_{t+1}}$ where $W_t = c_t + u_t p_t$, c_t is the number of units of the risky asset, u_t is the number of units of the risky asset, p_t is the price in round t of the risky asset, and ρ is a measure of risk aversion. If the total return of the risky asset (including the dividend) is normally distributed, then subject *i*'s demand for the risky asset is:

$$x_{it}(p_t) = \frac{\mathrm{E}_t[p_{t+1} + d_t] - p_t(1 + r)}{\rho\sigma^2}$$

When $x_{it}(p_t) = 0$, we have

$$p_{it}^* = \frac{\mathrm{E}_t[p_{t+1} + d_t]}{1 + r}$$

so under these (admittedly strong) assumptions our fitted values $\widehat{y_{it}} = Z_{it}\hat{\gamma}$ can be thought of as an approximation of subject i's beliefs regarding the present value of the risky asset. This expression can be generalized to reflect non-myopic plans. The assumption of CARA utility and normally distributed returns is equivalent to assuming that subjects have mean-variance preferences; see e.g. (10), pages 36-37.

Results. Columns 1 and 2 of Table S7 show the direct relationship on valuation of NAcc activity, and returns and dividend yield respectively. Column 3 shows that a 1 standard deviation change in our measure of NAcc activity is associated with a 1.1% increase in willingness to pay for the risky asset, after controlling for return and expected dividend yield.

Motivated by theoretical and experimental research that focuses on asymmetries among market participants as an important factor in driving bubbles, we divided subjects across all experiments into earning terciles. The model in Column 4 interacts the tercile of earnings with NAcc activity, and adds additional controls including the subject's lagged average orders and share position as well as indicators for each 5-round block in the experiment. The model in Column 5 adds a control variable that measures the subject's trading behavior. In many rounds, subjects respond either only "Buy" or only "Sell" to the stimulus prices, so dropping these rounds might result in a considerable loss of power. We therefore code the highest “bin” to which subjects responded “Buy ” from 0 to 5, with no buy response in the round coded as 0, and by coding the lowest “bin” to which subjects responded “Sell” from 1 to 6, with no sell response in the round coded as 6. We then calculated the variable “Buy-Sell midpoint” in round *t* by taking the average of these two numbers. This variable is a rough measure of the subject’s policy in a given round. In addition, this model adds additional controls for neural activity extracted from ROIs in the right anterior insula, the amygdala, the right temporoparietal junction and the left dorsolateral prefrontal cortex. These variables control for the possibility that variations in neural activity across the whole brain, rather than in the NAcc alone, are driving the results. The coefficient estimates from model 5 show that in the lowest earning subjects, a 1-standard deviation change in our measure of NAcc activity is associated with an approximately 2.6% increase in willingness-to-pay for the risky asset a number that is both statistically and economically meaningful. More accurate measures of NAcc activity are likely to improve the precision of this estimate.

Our results concerning the influence of NAcc activity on behavior are robust to different specifications of the dependent variable. Results of roughly the same significance level and magnitude are achieved when we perform: 1) Linear regressions where the dependent variable is the buy-sell midpoint. 2) Tobit regressions where the dependent variable is each subjects’ buy orders in a given round, normalized by the prior round’s price; alternatively we can use sell orders. 3) Ordered probit regressions where the dependent variable is the bin chosen, again using either the maximum “Buy” response or minimum “Sell” response.

Supplementary Tables and Figures.

	Subject Type			
	Behavioral (n = 276)		fMRI (n = 44)	
Variable	Mean	Std. dev.	Mean	Std. dev.
VTCRI	0.03	0.18	1.00	0.00
Sex	0.46	0.50	0.45	0.50
Asian	0.70	0.45	0.08	0.27
Black	0.02	0.14	0.07	0.26
White	0.27	0.44	0.85	0.36
Age	23.15	4.64	28.43	10.40
Quiz	3.87	1.27	3.43	1.45
Payout	$20.83	5.29	$21.09	5.19
Trades	19.46	9.03	18.34	10.19

Table S1. Subject composition, summary statistics. VTCRI: 1 if subjects participated at Virginia Tech Carilion Research Institute; 0 if subjects participated at UCLA**. Sex:** 0 if Female, 1 if Male**. Quiz:** number of correct answers on the pre-trade quiz. **Payout:** Earnings for participating in the trading experiment, excluding show-up fees. **Trades:** number of times a subject bought or sold in the experiment.

Variable	N(obs)	Mean	Std. Dev.	25%	50%	75%
Price	800	27.797	19.608	15.965	20.005	30.255
Price (max)	16	60.416	35.260	30.810	64.300	71.275
Price (min)	16	13.563	0.687	13.075	13.525	13.760
Price (final)	16	14.717	1.648	13.940	14.125	14.810
Volume	800	0.398	0.126	0.300	0.400	0.455
Rounds with Price >14	16	0.938	0.051	0.920	0.940	0.970
RAD	16	1.050	0.661	0.449	1.090	1.342
RD	16	1.047	0.661	0.446	1.088	1.339

Table S2. Market summary statistics. Price(all): all price observations; Price(max), Price(min) and Price(final) are the maximum, minimum, and final round prices in each session, respectively. Volume (all) is the normalized volume in each session, shown as the fraction of subjects who traded in each round. RAD: Relative Absolute Deviation; RD: relative deviation (see text for details).

Variable	(1) Payout	(2) Dependent Variable Total trades	(3) Quiz score
Sex	41.60	2.324*	0.477***
	(48.61)	(1.271)	(0.156)
VTCRI	65.86	0.923	-0.327
	(68.03)	(2.208)	(0.299)
Quiz Score	74.56**	0.539	
	(30.09)	(0.634)	
Black	-15.40	3.503	-1.295*
	(157.1)	(3.556)	(0.658)
Asian	73.80	3.728**	0.0298
	(54.17)	(1.730)	(0.207)
Total trades	-14.41***		
	(3.839)		
Cancelled trades	-5.972		
	(5.153)		
Constant	2,021***	13.63***	3.662***
	(68.96)	(2.818)	(0.152)
Observations	317	317	317
R-squared	0.093	0.061	0.081
Number of session	16	16	16
Session FE	Yes	Yes	Yes
Robust SE	Yes	Yes	Yes

Table S3. Determinants of subject behavior. Fixed-effects regressions**. Sex:** 0 if female, 1 if male. **VTCRI:** subjects participated at Virginia Tech Carillion Research Institute. **Total trades:** number of buy and sell transactions. **Cancelled trades:** trades cancelled either because the subject tried to sell and had 0 units of the risky asset available, or because the subject responded buy to a price that was greater than a price to which the subject responded sell. Robust standard errors in parentheses. *** p<0.01, ** p<0.05, * p<0.1.

Binary Variables								
Thresholds: p-value FWE 0.05; Cluster Extent k>5						**peak MNI coordinates**		
Variable	**Region**	**R/L**	**Brodmann Area**	**Voxels**	**Peak T**	**x**	**y**	**z**
Bought	Ventral Striatum	R/L	25	8	6.46	-14	8	-14
Sold	Ventral Striatum	R/L	25/47	206	9.05	10	8	-6
	Inferior Temporal Gyrus	R	19	10	6.87	46	-76	-6
	Inferior Frontal Gyrus	L	6/9	72	6.18	-50	8	22
	Orbitofrontal cortex	R	10/11/32	103	5.66	22	48	-10
	Inferior Frontal Gyrus	L	46	12	5.65	-42	32	14
	Inferior Parietal Lobule	L	40	16	5.64	-58	-32	46
	Cuneus	R	17	9	5.30	14	-88	2
	Anterior Cingulate Cortex	R	9/32	11	5.18	10	36	22
Thresholds: p-value: Uncorrected 0.005; Cluster Extent k>5								
Bought-Sold	Middle Frontal Gyrus	R	9	18	3.15	38	8	34
Sold-Bought	No significant clusters							

Parametric Modulator Variables								
Thresholds: p-value: Uncorrected 0.005; Cluster Extent k>5						**peak MNI coordinates**		
Variable	**Region**	**R/L**	**Brodmann Area**	**Voxels**	**peak T**	**x**	**y**	**z**
EDiv	Inferior Parietal Lobule	L	40	30	3.76	-54	-48	42
	Superior Temporal Gyrus	R	22/39	8	3.33	62	-64	14
	Inferior Parietal Lobule	R	40	28	3.25	62	-48	46
	Superior Temporal Gyrus	R	22	10	-3.04	58	8	-2
	Cuneus/Precuneus	R		9	-3.32	18	-84	50
	Middle Frontal Gyrus	L	6	9	-3.55	-50	0	46
	Precuneus	L	19	30	-3.75	-14	-84	46
	Ventral Striatum/ Anterior Cingulate Cortex	L	11/25/32	70	-4.07	-14	12	-14
Return	Superior Temporal Gyrus	R	19/22/39	23	2.70	54	-56	14

Table S4. GLM Results. Bought: indicator for "You Bought" message, convolved with a hemodynamic response function. **Sold:** indicator for "You Sold" message, convolved with a hemodynamic response function. **EDiv:** expected dividend yield (parametric modulator) for the risky asset in round *t*. **Return:** return for the risky asset in round *t*.

Neurosynth Reverse Inference: MNI (12,8,-8)		
Feature	**z-score**	**post. prob.**
reward	19.55	0.92
rewards	13.17	0.92
incentive	11.6	0.93
outcome	11.6	0.87
money	11.13	0.92
anticipation	10.41	0.89
monetary	10.32	0.9
outcomes	9.74	0.88
win	9.13	0.92
feedback	7.95	0.82

Table S5. Neurosynth reverse inference. Showing the 10 features with highest z-score of 525 entries. The table shows terms that appear with high frequency from the 167 studies in the Neurosynth database that report activation within 6 mm of MNI coordinates (12, 8, -8).
Downloaded from http://neurosynth.org/locations/12_8_-8 on July 10, 2013.

	Model			
Dependent Variable is Earnings ($)	**(1)**	**(2)**	**(3)**	**(4)**
NAcc-Buying	-13.49***		-11.06***	-12.47***
	(3.645)		(3.224)	(3.369)
Insula-Selling		11.59***	8.236**	8.053**
		(3.888)	(3.147)	(3.172)
Quiz Score			0.594	0.263
			(0.479)	(0.322)
Black				-8.397**
				(3.538)
White				-0.711
				(3.46)
Sex				0.0456
				(1.291)
Constant	21.65***	19.98***	18.76***	20.82***
	(0.78)	(0.869)	(1.602)	(3.813)
Observations	41	41	41	39
R-squared	0.273	0.215	0.417	0.538

Notes: Robust standard errors in parentheses. *** p<0.01, ** p<0.05, * p<0.1.

Table S6. Brain-behavior associations in the NAcc and the insula predict task performance. OLS estimates. **NAcc-Buying:** relationship between NAcc activity in the 6mm-radius ROI spheres centered at MNI (±12,8,-8) and subsequent buying. **Insula-Selling** relationship between insula activity in the 6mm radius sphere centered at MNI (36,24,2) and subsequent selling. **Sex:** 0 if female, 1 if male.

	Model				
Variable	**(1)**	**(2)**	**(3)**	**(4)**	**(5)**
NAcc	0.008		0.011**	-0.001	0.002
	(0.005)		(0.005)	(0.005)	(0.005)
Low Earns*NAcc				0.037***	0.026***
				(0.011)	(0.009)
Return		0.026***	0.028***	0.020**	0.001
		(0.009)	(0.009)	(0.009)	(0.008)
Dividend Yield		0.022*	0.021	0.047**	0.039**
		(0.013)	(0.013)	(0.023)	(0.016)
Buy-sell midpoint					0.079***
					(0.012)
Units				yes***	yes*
Units=0 (Indicator)				n.s.	n.s.
4 ROIs: rAIns, Amyg, rTPJ, lDLPFC					n.s.
Constant	1.000***	1.001***	1.002***	0.908***	0.932***
Low Earns (Indicator)				0.056***	0.062***
Subject FE	Yes	Yes	Yes	Yes	Yes
5 round dummies	No	No	No	Yes	Yes
Cluster level	Subject	Subject	Subject	Subject	Subject
Observations	1745	1829	1745	1745	1745

Table S7. Determinants of valuation for the risky asset. Interval regression estimates. The dependent variable is $[a_{it},b_{it}]$ where a_{it} is the maximum stimulus price to which subject i responded "Buy" in round *t*, and b_{it} is the minimum price to which subject *i* responded "Sell" in round *t*. All independent variables are lagged. NAcc: mean BOLD response in the 24-voxel bilateral Nucleus Accumbens ROI centered at MNI (±12,8,-8). Low Earns: Indicator for subjects in the lowest third of the earnings distribution. Buy-sell midpoint: the midpoint between buy and sell orders. Buy-sell midpoint is the average of the previous round's maximum buy and minimum sell orders by bins, numbered from 1 to 5. Missing buy orders were coded as 0 and missing sell orders coded as 6. Units: units of the risky asset. rAIns: right Anterior Insula. Amyg: Amygdala. rTPJ: right temporoparietal junction. lDLPFC: left dorsolateral prefrontal cortex.

*** p<0.01, ** p<0.05, * p<0.1. Cluster-corrected standard errors in parentheses.

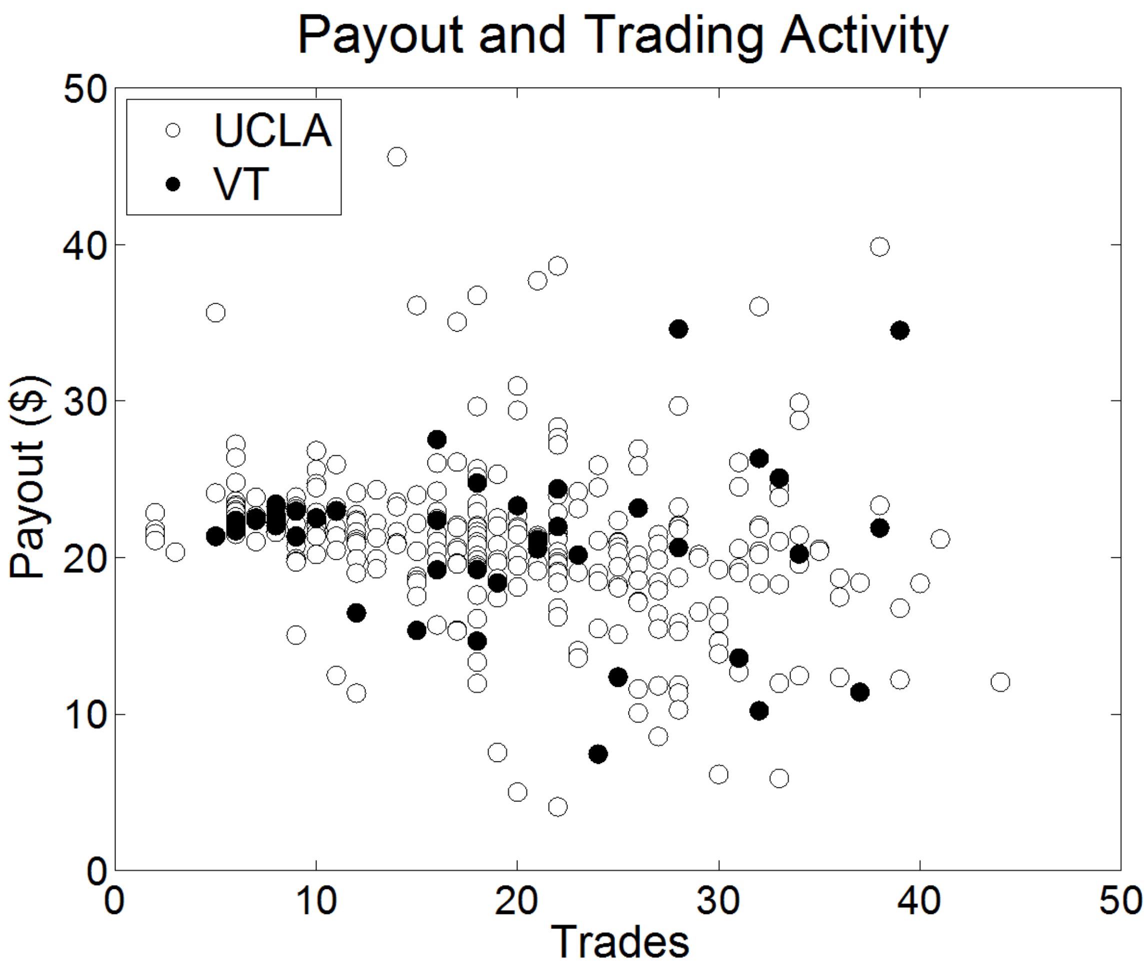

Figure S1. Payouts and Trading activity. Each circle represents an individual participant. The light circles are UCLA (behavioral) subjects, and the shade circles represent VT (fMRI) subjects. The x-axis shows the number of trades the subject made, and the y-axis is the subject's payout in the experiment. There are no significant differences between the two groups in either the number of trades ($p=0.339$, Wilcoxon rank-sum test; $p = 0.3223$, Kolmogorov-Smirnov test) or in payouts ($p = 0.2164$, Wilcoxon rank-sum test; $p = 0.1551$, Kolmogorov-Smirnov test).

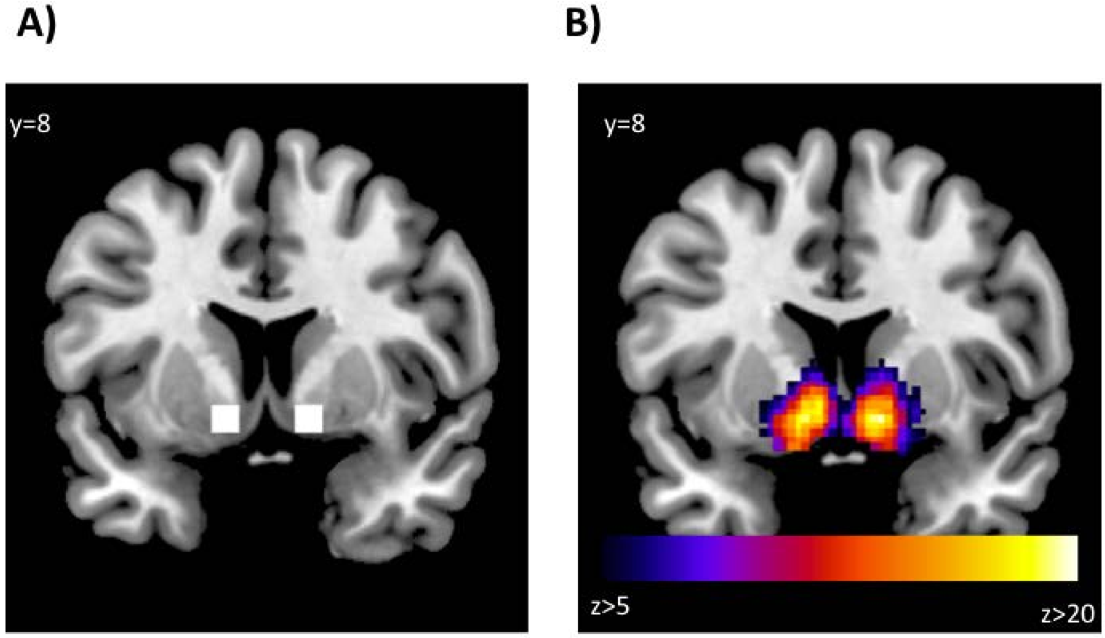

Figure S2. A) NAcc ROI: Two 6mm-radius spheres centered at MNI (±12,8,-8) in the nucleus accumbens. There are 12 voxels in each sphere. B) **Neurosynth reverse inference feature map.** This reverse inference map shows z-statistics that measure the likelihood that the term "reward" will be associated with a reported activation in a given brain region**.** Image downloaded from http://neurosynth.org/features/reward on July 10, 2013.

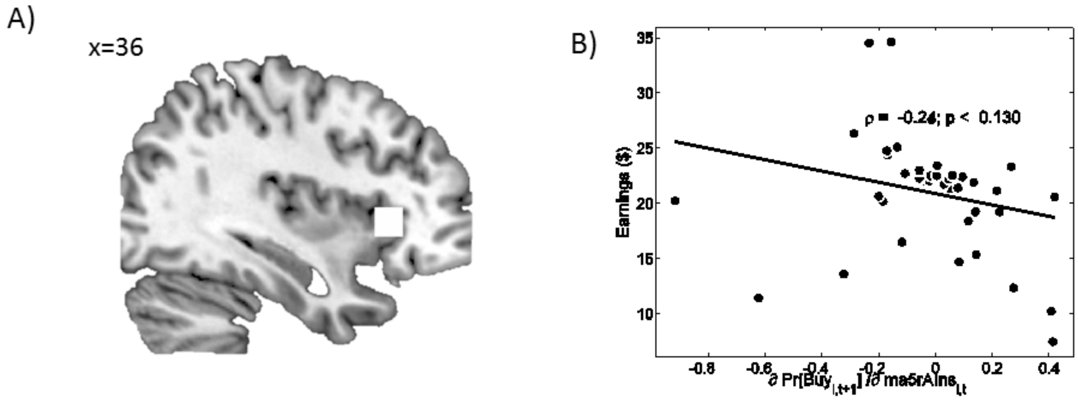

Figure S3. A) Insula ROI: A 6mm-radius sphere centered at MNI (36,24,2) in the right anterior insula. **B)** Earnings compared with the estimated brain-buying relationship in the insula. We do not find a statistically significant association between earnings and the degree to which neural activity in the insula predicts buying in the next trading round.

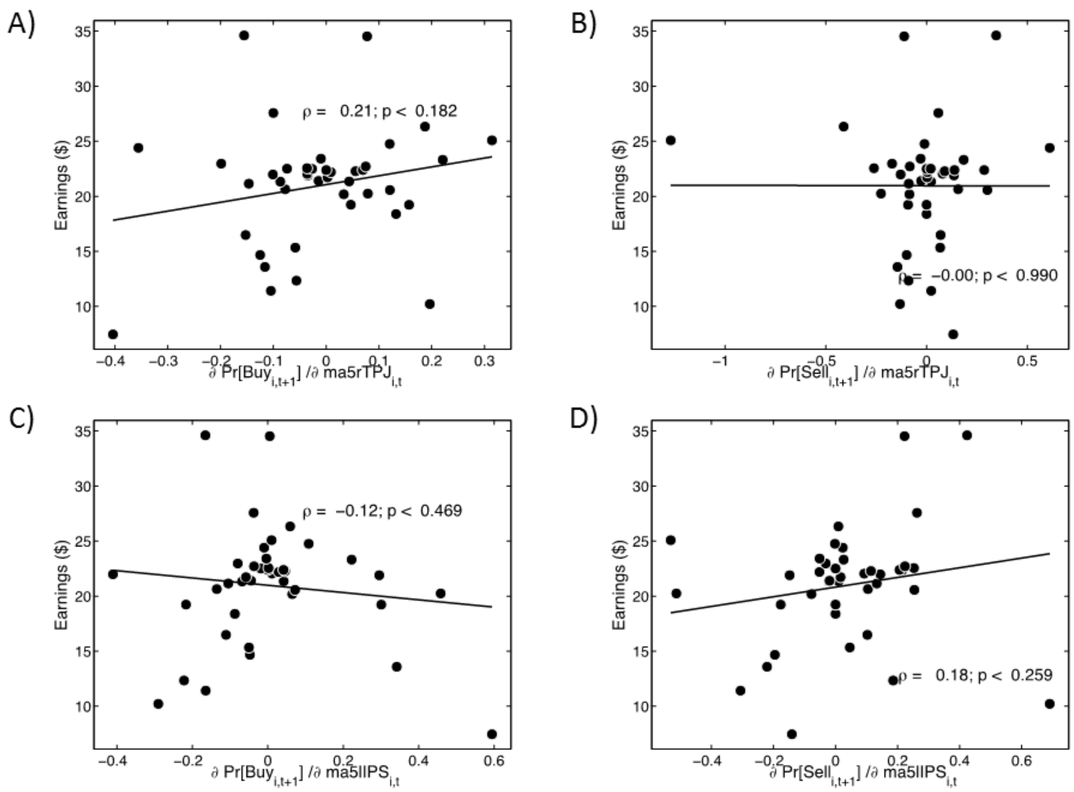

Figure S4. Neurobehavioral control regions. A) Earnings compared with the estimated brain-buying relationship in the rTPJ. **B)** Earnings compared with the estimated brain-selling relationship in the rTPJ. **C)** Earnings compared with the estimated brain-buying relationship in the lIPS. **D)** Earnings compared with the estimated brain-selling relationship in the lIPS.

<u>INSTRUCTIONS</u>

This experiment is about economic decision-making in an experimental market. If you make good decisions, you might earn a considerable amount of money, which will be paid to you in US dollars at the end of the experiment. The experiment will consist of a series of 50 trading periods in which you will have the opportunity to buy or sell shares of an asset that can yield payments in the future.

There are two assets in this experiment: CASH (experimental currency units) and STOCK. You begin with 100 units of CASH and 6 shares of STOCK.

STOCK is traded in a market each period among all the experimental subjects, in units of CASH. When you buy STOCK, the price you agreed to pay is deducted from your amount of CASH. When you sell STOCK the price you sold at is added to your amount of CASH.

Each period, every unit of STOCK earns a low or high dividend of either 0.40 CASH per unit or 1.00 CASH per unit. These dividend payments are equally likely, and are the same for everyone in each period. However, the dividend in each period does not depend on whether the previous dividend was low or high.

CASH earns a fixed interest rate of 5% each period.

At the end of the 50 periods of trading, each unit of STOCK is automatically traded in for 14.00 CASH. Then your experiment CASH units are converted to US dollars at a rate of 100 CASH = $1 US, to determine how much you will be paid at the end of the experiment.

For example, suppose in a period you have 120 units of CASH and 5 units of STOCK, and the dividend is 0.40 per unit of stock. Then your new CASH amount would be a 5% increase times 120 (a gain of 6) and total dividends of 0.40 x 5 = 2. Your total CASH would therefore increase by 6 + 2 = 8 units. Notice that keeping CASH will earn a return (5% per period) and using CASH to buy units of STOCK will also yield dividend earnings. If you are trying to earn the most money you might think about whether keeping CASH or buying STOCK creates more earnings.

<u>Trading</u>

In each period you will be shown a series of 5 prices. You have 2 seconds to make a decision. In response to each price, you must quickly state whether you would BUY 1 unit of stock or SELL 1 unit of stock at that price, or HOLD your current position (not buying or selling). If you do not enter a response in time the default choice that will be made for you is HOLD.

The highest price for which you select BUY and the lowest price for which you select SELL will be entered as “limit orders”. A limit order to buy at a price of 17, for example, means you would like to buy at the price of 17 and *at any lower price*. Similarly, a limit order to sell at 11 means you would like to sell at the price of 11 and *at any higher price*.

After all participants enter orders, a single market price P* is determined which matches the number of people who would like to buy at that price with the same number of people who would like to sell. (That is, the number of limit orders to buy at price P* or higher equals the number of limit orders to sell at price P* or lower.) Participants who responded BUY to prices at or above P* will buy one unit of STOCK at P*. Participants who responded SELL to prices at or below P* will sell one unit of STOCK at P*.

If there are ties in the number of traders who want to buy and sell at exactly P* then a random choice determines which traders will actually BUY or SELL. If there are no orders to BUY, then there are no trades and the last price is reported as the minimum price at which traders would SELL, and if there are no orders to SELL the reported price is the maximum price at which traders would BUY.

<u>Trading restrictions:</u>

Saying that you will BUY at a higher price than you are willing to SELL at is considered a trading mistake, and is not allowed. If this happens your orders will be canceled for that trading period (the same as choosing HOLD).

Also, you must have enough CASH to pay the price of STOCK you would like to BUY. If you do not have enough CASH to buy stocks, your order will be canceled. You also cannot SELL a share of stock if you have no available shares.

<u>Using the keyboard to trade:</u>

Enter SELL by pressing 1, HOLD by pressing 2, and BUY by pressing 3 on your keyboard.

<u>Trading practice:</u>

Before the experiment begins you will have the opportunity to practice trading during 3 practice trading periods. Your decisions during these practice rounds will not count towards your payment for the experiment.

<u>Experiment preview:</u>

Each trial consists of the following screens POSITIONS, ORDER ENTRY, TRADING RESULTS, and DIVIDENDS and INTEREST. Each of these is shown below. In between each screen you will briefly see a fixation cross.

The POSITIONS screen shows your current holdings of STOCK and CASH, the most recent traded price for STOCK, and a price history graph.

The ORDER ENTRY screen is where you enter limit orders. You will see a price. Press 1, 2, or 3 to SELL, HOLD or BUY. You will see this screen 5 times per period.

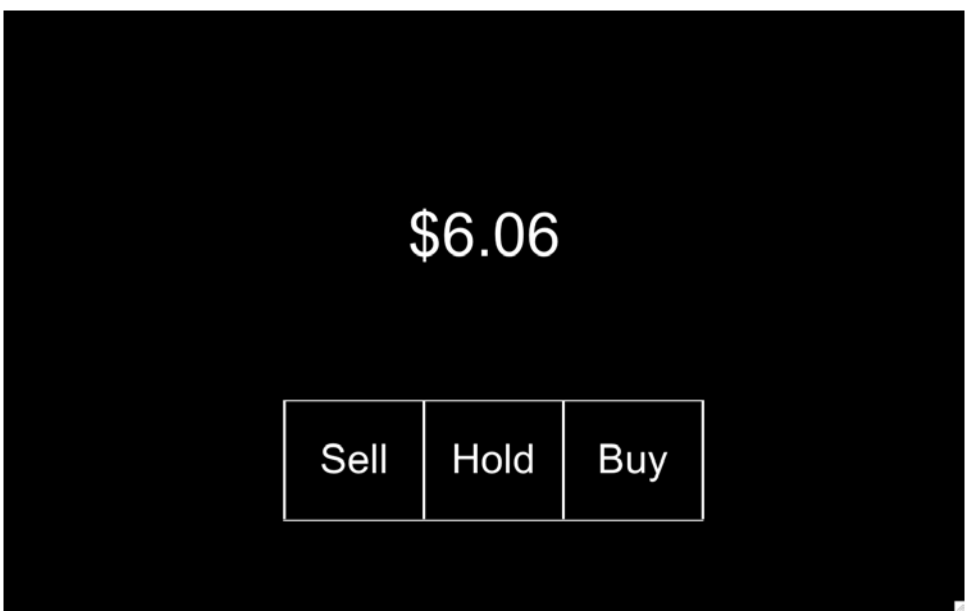

The TRADING RESULTS screen shows the market price and whether you bought sold, or held that trading period.

The DIVIDENDS and INTEREST screen shows the total dividends you earned that trading period from shares of stock, and the INTEREST you earned that round on your CASH holdings.

Quiz [Correct answers are *in italics*.]

Subject ID: ___________
Session: ___________

1. During order entry you press BUY in response to a price of 8.52 and SELL in response to a price of 7.89. What will happen to your orders for that period?
   a. They'll be entered as usual
   b. They'll be canceled

2. During order entry the <u>highest</u> price to which you respond BUY is 16.78 and the <u>lowest</u> price to which you respond SELL is 17.22. The market price is 16.56 for that period. You will:
   a. BUY one unit at 16.78
   b. BUY one unit at 16.56
   c. SELL one unit at 16.56
   d. SELL one unit at 17.22
   e. Not trade

3. You have 200 units of CASH at the start of a trading period and no STOCK. You do not trade that period. How much CASH do you have at the beginning of the next period?
   a. 200
   b. 205
   c. 210
   d. 190

4. Your account has 5 STOCK and 100 CASH at the start of a trading period, and you do not BUY or SELL during that period. The dividend for that round is 1.00. How much CASH do you have at the start of the next round?
   a. 105
   b. 110
   c. 100
   d. 114

5. After the final trading period, you have 4 remaining units of STOCK. The market price in the final period is 29. How many units of experiment CASH do you receive in exchange for your STOCK?
   a. 4
   b. 29
   c. 56
   d. 116

References

1. T. Stockl, J. Huber, M. Kirchler, Bubble measures in experimental asset markets. *Experimental Economics* **13**, 284 (Sep, 2010).
2. M. Kirchler, J. Huber, T. Stockl, Thar She Bursts: Reducing Confusion Reduces Bubbles. *American Economic Review* **102**, 865 (2012).
3. K. J. Friston *et al.*, Event-Related fMRI: Characterizing Differential Responses. *NeuroImage* **7**, 30 (1998).
4. T. Yarkoni, R. A. Poldrack, T. E. Nichols, D. C. Van Essen, T. D. Wager, Large-scale automated synthesis of human functional neuroimaging data. *Nature methods* **8**, 665 (2011).
5. K. Preuschoff, P. Bossaerts, S. R. Quartz, Neural differentiation of expected reward and risk in human subcortical structures. *Neuron* **51**, 381 (Aug 3, 2006).
6. N. Tzourio-Mazoyer *et al.*, Automated anatomical labeling of activations in SPM using a macroscopic anatomical parcellation of the MNI MRI single-subject brain. *Neuroimage* **15**, 273 (2002).
7. R. Saxe, N. Kanwisher, People thinking about thinking people: the role of the temporo-parietal junction in "theory of mind". Neuroimage, **19**(4), 1835 (2003).
8. M. Piazza, P. Pinel, D. Le Bihan, and S. Dehaene. "A magnitude code common to numerosities and number symbols in human intraparietal cortex." *Neuron* **53**(2), 293 (2007).
9. J. M. Wooldridge, *Econometric Analysis of Cross Section and Panel Data*. (MIT Press Books, Cambridge, MA, 2003).
10. K. Back, *Asset pricing and portfolio choice theory*. (Oxford University Press, USA, 2010).